



Core structure of a screw dislocation in the b.c.c. lattice and its relation to slip behaviour of α -iron

S. Takeuchi

To cite this article: S. Takeuchi (1979) Core structure of a screw dislocation in the b.c.c. lattice and its relation to slip behaviour of α -iron, Philosophical Magazine A, 39:5, 661-671, DOI: [10.1080/01418617908239296](https://doi.org/10.1080/01418617908239296)

To link to this article: <http://dx.doi.org/10.1080/01418617908239296>



Published online: 27 Sep 2006.



Submit your article to this journal [↗](#)



Article views: 48



View related articles [↗](#)



Citing articles: 46 View citing articles [↗](#)

Core structure of a screw dislocation in the b.c.c. lattice and its relation to slip behaviour of α -iron

By S. TAKEUCHI

The Institute for Solid State Physics, The University of Tokyo,
Minato-ku, Tokyo 106, Japan

[Received 21 September 1978 and accepted 17 December 1978]

ABSTRACT

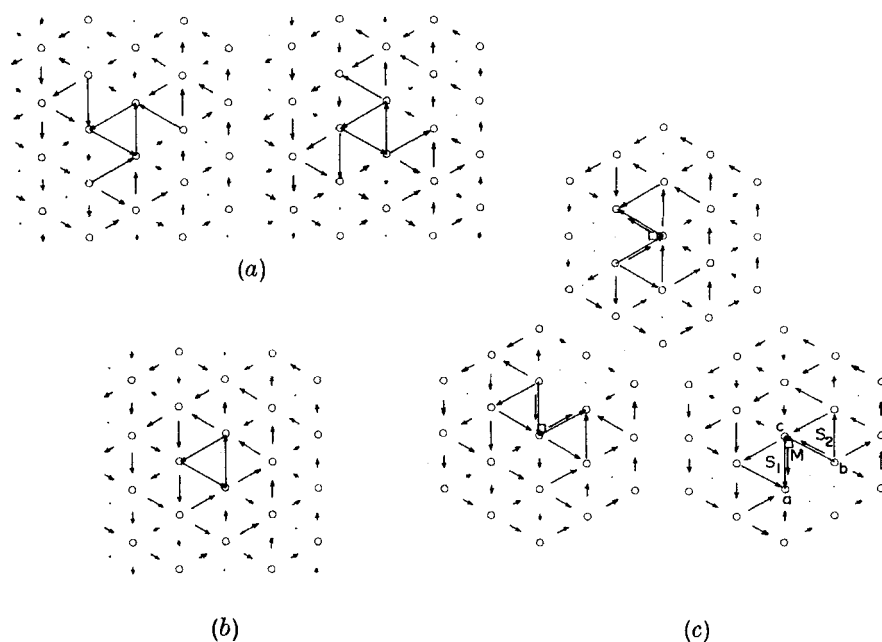
Using various interatomic row potentials, the atomistic structure of the core of a screw dislocation in the b.c.c. lattice has been computed. Stable core structure is either of a degenerate or a non-degenerate type depending on the shape of the interatomic row potential; the criterion for the core type is presented. A non-degenerate stable core is always accompanied by the existence of a metastable core structure of a split type. Characteristic features of slip in α -iron are reasonably interpreted based on the translation of a non-degenerate core over a camel-hump Peierls potential.

§ 1. INTRODUCTION

Atomistic studies of the core structure of a screw dislocation in the b.c.c. lattice have been made using various interatomic potentials (see the review by Vitek 1974). Most of the results show that the stable core structure of a screw dislocation has two energetically equivalent configurations, as first pointed out by Vitek (1970). Such a core structure is called 'degenerate'. An example of a degenerate core structure is shown by the conventional displacement map (Vitek, Perrin and Bowen 1970) in fig. 1(a), where arrows indicate magnitude and sense of relative displacements in the direction of the Burgers vector, with respect to the perfect lattice, between two neighbouring atomic rows. Under an applied stress higher than the Peierls stress, computer simulation shows that the degenerate core moves in a zigzag manner, changing the core type alternately between the two configurations of a degenerate core (Basinski, Duesbery and Taylor 1971, Minami, Kuramoto and Takeuchi 1972, 1974, Duesbery, Vitek and Bowen 1973, Kuramoto, Minami and Takeuchi 1974, Hübner 1975, Vitek 1976) and the resultant slip plane is $\{112\}$ in many cases.

Using interatomic row potentials composed of the first- and the second-order Fourier components, Minami *et al.* (1974) have shown that, in addition to the degenerate core structure, a screw dislocation can take a non-degenerate core structure, as shown in fig. 1(b), depending on the potential shape. Furthermore, in the case of the non-degenerate core, a trebly degenerate metastable core structure such as shown in fig. 1(c) also exists; we have called this 'the split core structure'. The dislocation centre, which is determined from the strain field far from the core, in the split core is near an atomic row (Takeuchi and Kuramoto 1975) as indicated by square marks in fig. 1(c).

Fig. 1



Displacement maps (see text) showing three core types of a screw dislocation : (a) doubly degenerate stable core ; (b) non-degenerate stable core ; and (c) trebly degenerate metastable core structure.

Mechanical testing on single crystals of iron and its alloys have shown that the yield stress is a minimum when the resolved shear stress is a maximum on a $\{110\}\langle 111 \rangle$ system (e.g. Spitzig and Keh 1970, Sestak and Seeger 1971). Recent experiments at helium temperature on high-purity iron single crystals ($RRR \sim 3000$) also exhibits the same results (K. Kitajima, Y. Aono, H. Abe and E. Kuramoto 1978, private communication). Microscopic observations have shown that slip planes tend to confine themselves to $\{110\}$ planes as the temperature is lowered (e.g. Takeuchi, Taoka and Yoshida 1969). These results indicate that $\{110\}$ glide is most favourably operative in iron and its alloys. Also, the well-known $\{112\}$ asymmetry of slip is commonly observed in iron and its alloys (e.g. Takeuchi *et al.* 1969), as well as other b.c.c. metals (see reviews by Hirsch 1968, Christian 1970). Another interesting feature is that the curves of yield stress versus temperature for iron whiskers (Conte, Groh and Escaig 1968), Fe-Ti alloys (Leemans and Fine 1973), high-purity polycrystalline iron (Tseng and Tangri 1977, Matsui, Moriya, Takaki and Kimura 1978) and single crystals (Quesnel, Sato and Meshii 1975, Kitajima *et al.* 1978, private communication) show a convex region between 150 and 250 K. These characteristic features of deformation behaviour of α -iron are more easily understood on the basis of the non-degenerate core, rather than the degenerate core usually assumed by other authors.

In this paper, it will be shown that for various interatomic row potentials the stable core structure can be of non-degenerate type, which is always accompanied by a metastable split-type configuration.

§ 2. INTERATOMIC ROW POTENTIALS

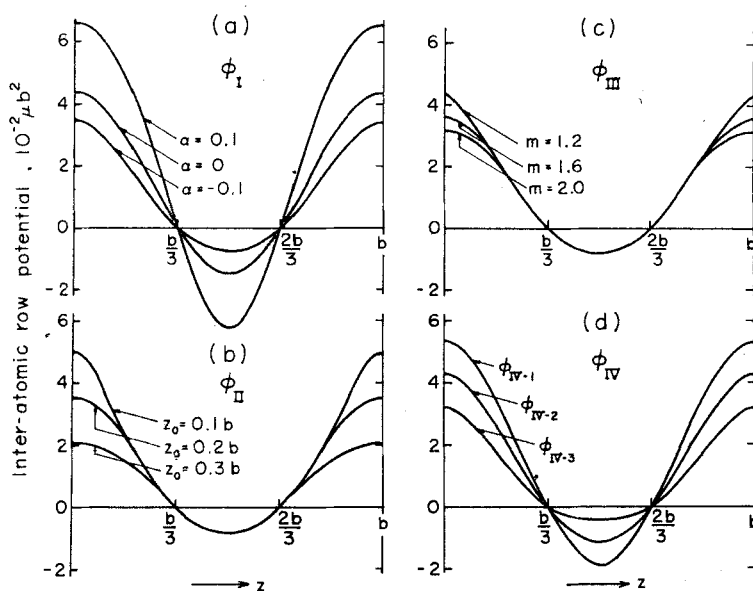
The interatomic row potential is assumed to be a function only of the relative positions, in the direction of the atomic row, of atoms in two $\langle 111 \rangle$ atomic rows. No further interaction than the nearest-neighbour atomic rows is considered. This type of potential is particularly useful in the treatment of a straight screw dislocation for obvious reasons. The potential has a periodicity of an interatomic spacing in atomic rows, which corresponds to the strength of the Burgers vector \mathbf{b} . It seems natural to assume that it has a maximum and a minimum at $z=0$ and $z=b/2$, respectively, where z is the difference in atomic positions. We have used the following various types of potentials, where the potential energy is defined for a unit length of a pair of atomic rows and the origin is taken at the perfect lattice positions, i.e. at $z=b/3$ and $2b/3$.

(I) Potentials composed of the first- and the second-order Fourier components and expressed by

$$\phi_I = \frac{\mu b^2}{2\sqrt{3}\pi^2(1-4\alpha)} \left[\cos \frac{2\pi z}{b} - \alpha \cos \frac{4\pi z}{b} + \frac{1}{2} - \frac{\alpha}{2} \right], \quad (1)$$

where μ is the shear modulus for the shear in the direction of atomic rows and α is a parameter of the potential. α has been changed between -0.2 and $+0.1$. ϕ_I curves for three values of α are shown in fig. 2 (a). This type of potential has originally been used by Suzuki (1970) and later by the present author and his colleagues (Minami *et al.* 1974, Kuramoto *et al.* 1974).

Fig. 2



Various interatomic row potentials per unit length of a pair of atomic rows used in the present calculation: (a) ϕ_I potentials (eqn. (1)); (b) ϕ_{II} potentials (eqn. (2)); (c) ϕ_{III} potentials (eqn. (3)); and (d) ϕ_{IV} potentials (eqns. (4) to (6)).

(II) Potentials with concave and convex parabolas joined together smoothly, which are expressed by

$$\phi_{II} = \begin{cases} k[\{1 - b/(2z_0)\}(z/b)^2 - z_0/(2b) + 2/9] & \text{for } 0 \leq z \leq z_0, \\ k[(z/b)^2 - (z/b) + 2/9] & \text{for } z_0 \leq z \leq b - z_0, \\ k[\{1 - b/(2z_0)\}(1 - z/b)^2 - z_0/(2b) + 2/9] & \text{for } b - z_0 \leq z \leq b, \end{cases} \quad (2)$$

with $k = \mu b^2/2\sqrt{3}$. z_0 is a parameter representing an inflection point of the potential and has been varied between $0.1b$ and $0.3b$. Some potential curves of eqn. (2) are shown in fig. 2 (b).

(III) Potentials with a parabolic bottom and with a peak of the type $-z^m$ ($m \leq 2$), which are connected at $z_1 = (9/40)b$ and $z_2 = (31/40)b$. The reason for the selection of these values will be mentioned later. They are expressed by

$$\phi_{III} = \begin{cases} k[-k_1(z/b)^m + k_2] & \text{for } 0 \leq z \leq z_1, \\ k[(z/b)^2 - (z/b) + 2/9] & \text{for } z_1 \leq z \leq z_2, \\ k[-k_1(1 - z/b)^m + k_2] & \text{for } z_2 \leq z \leq b, \end{cases} \quad (3)$$

with $k = \mu b^2/2\sqrt{3}$, $k_1 = 0.55(40/9)^{m-1}/m$ and $k_2 = 99/800m + 689/14\,400$. The parameter m has been varied between 1.1 and 2.0 . Some potentials of this type are presented in fig. 2 (c).

(IV) Higher-order polynomial functions defined for $0 \leq z \leq b$ and expressed by

$$\phi_{IV-1} = (2\sqrt{3}\mu b^2/3)[-|z/b - 0.5|^3 + 0.75(z/b - 0.5)^2 - 7/432], \quad (4)$$

$$\phi_{IV-2} = (\sqrt{3}\mu b^2/2)[-(z/b - 0.5)^4 + 0.5(z/b - 0.5)^2 - 17/1296], \quad (5)$$

$$\phi_{IV-3} = \sqrt{3}\mu b^2[-(z/b - 0.5)^4 + (2/3)|z/b - 0.5|^3 - 1/432]. \quad (6)$$

These potential curves are shown in fig. 2 (d).

§ 3. COMPUTATION

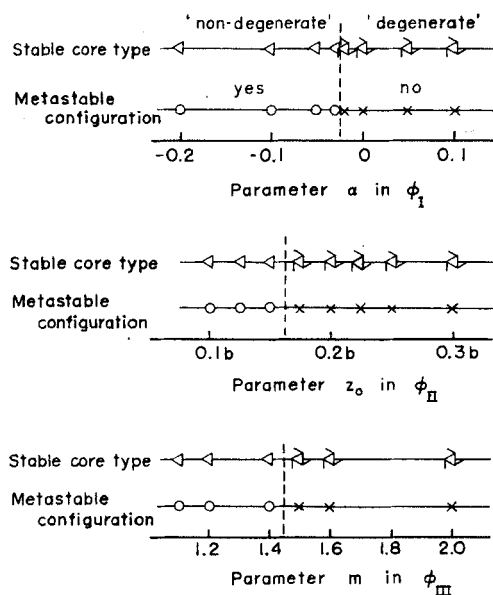
Computation procedure is the same as that in previous papers (Minami *et al.* 1974, Takeuchi and Kuramoto 1975). The size of the model crystal used was about $20b \times 20b$. The type of the stable core structure, degenerate or non-degenerate, has been studied by relaxing the initial displacements based on a linear elasticity solution whose centre is placed at a low-energy site (Suzuki 1968). The stability of the metastable configuration of the type shown in fig. 1 (c) has been examined by the following procedure. After a typical metastable configuration has been put in as an initial condition, the whole configuration has been relaxed in two steps; at first with three atomic rows, a , b , c , in fig. 1 (c), being fixed and then without any restriction. If the split configuration is not stable, the structure falls in a stable configuration during the second relaxation process.

For the case where the split configuration is stable, a Peierls potential from one stable position to another via a split metastable configuration has been calculated in an approximate way as in the previous paper (Takeuchi and Kuramoto 1975): Three atomic rows, a , b , c in fig. 1 (c), have been used as 'guide atomic rows' (Heinrich and Schellenberger 1971) to obtain energies of unstable configurations; i.e. coordinates of the three atomic rows have been stepwisely changed from those in a stable configuration at S_1 to those at S_2 through those in a metastable state at M , and the structural relaxation at each step has been performed by fixing the coordinates of the three rows. In this process a linearity between the dislocation position and the changes of the coordinates of the guide atomic rows has been assumed.

§ 4. RESULTS

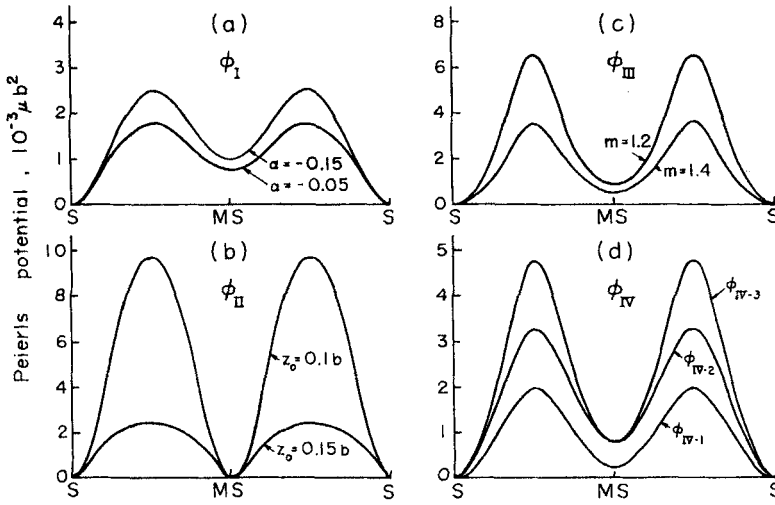
The results on the stable core type and the existence of the metastable configuration for ϕ_I , ϕ_{II} and ϕ_{III} potentials are shown diagrammatically in fig. 3. For all the ϕ_{IV} potentials, the stable-core type is the non-degenerate one and there exists the metastable split configuration. It is to be noted from these results that the non-degenerate core is always accompanied by the existence of the metastable split configuration and the degenerate core is always not so accompanied. Figure 4 shows Peierls potentials for the transition, a stable non-degenerate configuration \rightarrow a metastable split configuration \rightarrow

Fig. 3



Diagrams showing computed results of the dependence of parameters in ϕ_I , ϕ_{II} and ϕ_{III} potentials on: (1) the core type of stable configuration; and (2) existence of the metastable split configuration. Meanings of symbols indicated in top rows.

Fig. 4



Calculated Peierls potentials defined for a unit length of the dislocation between two stable positions via a split metastable configuration for : (a) ϕ_I potentials ; (b) ϕ_{II} potentials ; (c) ϕ_{III} potentials ; and (d) ϕ_{IV} potentials. Note that the ordinate scales are different between (a), (d) and (b), (c).

another stable non-degenerate configuration, for various potentials. The height and shape of the Peierls potential vary significantly with the change of the interatomic row potential. For the ϕ_{II} potential, the energies of the two configurations, non-degenerate and split configurations, are exactly the same ; so that the word 'metastable' is not appropriate in this case.

§ 5. DISCUSSION

5.1. Interatomic row potential model

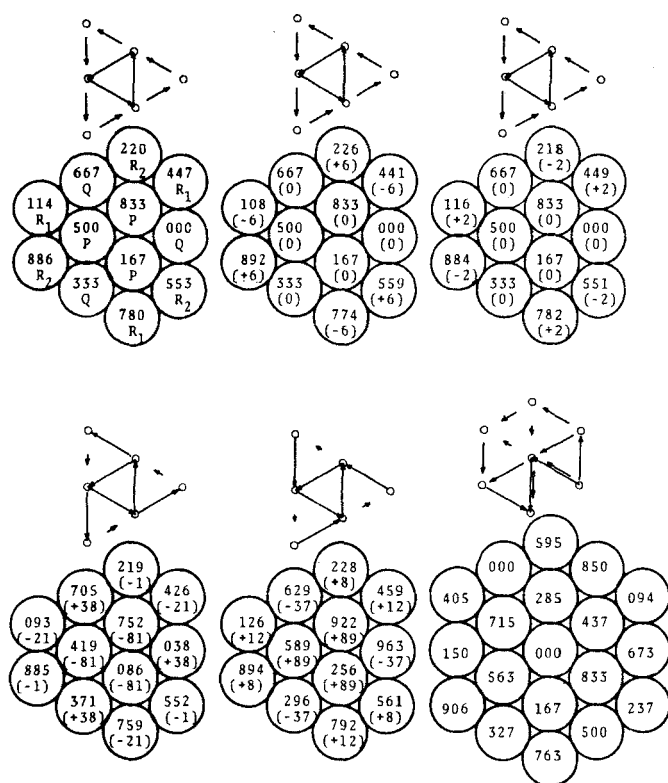
As shown in previous papers (Minami *et al.* 1974, Takeuchi and Kuramoto 1974), interatomic row potentials for many b.c.c. metals, which are calculated from interatomic potentials given in the literature (determined either empirically using elastic constants, sublimation energy, etc., for transition b.c.c. metals or based on the psuedo-potential theory for normal metals) have a maximum ranging from 0.025 to 0.05 μb^2 at $z=0$ and a minimum from -0.01 to -0.02 μb^2 at $z=b/2$. Thus, various hypothetical interatomic row potentials used in this paper will cover those potentials determined for real b.c.c. metals.

The interatomic row potential model is subject to some doubt if the neglect of the dilatational displacements of atomic rows at the screw dislocation core, although small compared with the displacements along the rows, may play a decisive role in the results (Vitek 1976). This weak point of the model will be much relieved by considering that our interatomic row potentials are defined by the interaction energy between a pair of atomic rows not for the rigid displacement parallel to the atomic rows but including a relaxation in the direction perpendicular to them in an average constraint

by surrounding atomic rows. As for a screw dislocation, z values for a few pairs of atomic rows are as small as $b/6$ and thus the separation of these pairs must be considerably increased; thus, for such small values of z , the interatomic row potentials are assumed to be defined for an increased separation of these atomic rows.

In any case, considering that the two-body interatomic potential description itself is not well founded for transition metals, the degree of approximation is not so important as the selection of the potential itself. In this situation it seems worthwhile to study various possibilities arising from systematically varied potentials by an approximate method rather than performing a more elaborate calculation using a definite hypothetical potential.

Fig. 5



Coordinates of atoms of central atomic rows of a screw dislocation represented by a unit of $10^{-3}b$ for: (a) linear elasticity solution; (b) non-degenerate core for $\phi_I(\alpha = -0.05)$; (c) non-degenerate core for $\phi_{II}(z_0 = 0.15)$; (d) degenerate core for $\phi_I(\alpha = 0)$; (e) degenerate core for $\phi_{II}(z_0 = 9/40) (\equiv \phi_{III}(m = 2.0))$; (f) metastable split configuration for $\phi_{III}(m = 1.4)$. In (b) to (e), differences from elasticity solution of (a) are shown in parentheses. A displacement map is also shown for each configuration to clarify the dislocation type.

5.2. Degenerate or non-degenerate core

Coordinates of atoms along atomic rows in the central region of a screw dislocation are shown in fig. 5 in units of $10^{-3}b$ for: (a) a linear elasticity solution; (b) a non-degenerate configuration for ϕ_I ($\alpha = -0.05$); (c) a non-degenerate configuration for ϕ_{II} ($z_0 = 0.15b$); (d) a degenerate configuration for ϕ_I ($\alpha = 0$); (e) a degenerate configuration for ϕ_{II} ($z_0 = 9/40$) or equivalently ϕ_{III} ($m = 2.0$); and (f) a split metastable structure for ϕ_{III} ($m = 1.4$). In (b) to (e), deviations from the elastic solution are indicated in parentheses. It is seen that non-degenerate configurations are very close to that of the linear elasticity solution. Compared with the elasticity solution, the degenerate configuration is characterized, as seen in (d) and (e), by an upward or downward displacement of three central atomic rows, P s in fig. 5 (a), and a downward or upward displacement of the next three atomic rows, Q s, as described already by others (Seeger and Wüthrich 1976, Wüthrich 1977). Thus, it can be understood that the criterion of the degeneracy of the dislocation may be the stability of the degenerate configuration for the above mode of perturbation, i.e. displacements of the P and Q atomic rows in the opposite directions. The energy change δE from the configuration of elasticity solution for an infinitesimal displacement δ_1 of the P atomic rows and $-\delta_2$ of the Q atomic rows, is written as

$$\delta E = 3[A\delta_1^2 + 2B\delta_1\delta_2 + C\delta_2^2], \quad (7)$$

where

$$\left. \begin{aligned} A &= \phi''(b/3 + \epsilon_1) + \phi''(b/6), \\ B &= \phi''(b/6), \\ C &= \phi''(b/6) + \phi''(b/2 + \epsilon_1) + \phi''(b/3 - \epsilon_2), \end{aligned} \right\} \quad (8)$$

with $\epsilon_1 = (b/2\pi) \tan^{-1}(\sqrt{3}/5) \simeq 0.053b$ and $\epsilon_2 = (b/2\pi) \tan^{-1}(\sqrt{3}/7) \simeq 0.039b$. For δE to be positive or for the non-degenerate configuration to be stable, the following inequalities must be satisfied simultaneously:

$$A > 0, \quad C > 0, \quad B^2 - AC < 0. \quad (9)$$

When this condition is not satisfied, the core structure will change to degenerate type.

For the potential ϕ_{III} , the inflection points of the potential, z_1 and z_2 , have been so selected that the interactions between atomic rows are harmonic except those between the P and Q atomic rows in fig. 5 (a), so that eqns. (8) and (9) are quite simplified. By solving inequalities of (9) for the ϕ_{III} potential, we obtain

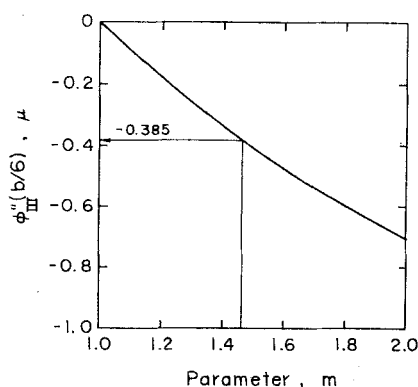
$$\phi_{III}''(b/6) > -2\mu/(3\sqrt{3}) \simeq -0.385\mu. \quad (10)$$

In fig. 6, the relation between $\phi_{III}''(b/6)$ and the parameter m is shown, which indicates that eqn. (10) holds for $m < 1.46$. This result is in accord with the range of the non-degenerate core type shown in fig. 3. For the potentials ϕ_{II} and ϕ_{IV} s, we can also readily show that the criterion of eqns. (8) and (9) is in agreement with the computed results of the core type.

For ϕ_I potentials, after solving eqns. (8) and (9), one obtains

$$-4.55 < \alpha < -0.018. \quad (11)$$

Fig. 6



Relation between the value of $\phi_{III}''(b/6)$ and the parameter m . The value of -0.385 is the critical value determined from eqns. (8) and (9).

In actual computation, the core type changes at a value between -0.02 and -0.03 , so that a slight deviation is found. This slight discrepancy is explained as follows: The criterion of eqns. (8) and (9) has been obtained starting from the configuration based on the linear elasticity solution, but the real equilibrium (not necessarily stable) non-degenerate structure for any assumed potential is not exactly the same as this, as seen in fig. 5 (b) and (c); the difference is characterized by a slight upward displacement of R_1 atomic rows and a downward displacement of adjacent R_2 atomic rows in fig. 5 (a). Thus, the value of ϵ_2 in eqn. (8) should be modified. The magnitude of the modification is, however, generally small ($\lesssim 0.01b$); therefore, eqns. (8) and (9) give a good criterion as demonstrated above.

Considering that terms other than $\phi''(b/6)$ in eqn. (8) are probably not much different from $\phi''(b/3) = \mu/\sqrt{3}$, the core type is influenced essentially by the value of $\phi''(b/6)$ or the curvature of the potential at $z=b/6$; roughly speaking, a large convex curvature at $z=b/6$ leads to the degenerate type and a small convex or a concave curvature to the non-degenerate type. A similar argument for the stability of the symmetric dislocation core has been given by T. Ninomiya (1974, private communication).

5.3. Existence of metastable split configuration

In the present results, a unique correspondence exists between the stable core type and the existence of the metastable split configuration. The split configuration is characterized by the configuration of three central atomic rows, a , b and c in fig. 1 (c), where the differences in coordinates between a and c , and b and c are $\pm b/6$ (see, also fig. 5 (f)). Thus the stability of this configuration also depends on the curvature of the potential at $z=b/6$ in a similar manner to the stability of the non-degenerate core. Therefore, the same tendency is expected between the core type and the stability of the split configuration for varying potentials, but the unique correspondence in fig. 3 may be fortuitous.

The shape and magnitude of the calculated Peierls potentials in fig. 4 depend sensitively on the shape of the interatomic rows potential; in particular, the height of the Peierls potential is not simply related to the height of the interatomic row potential as seen for ϕ_{II} and ϕ_{IV} potentials.

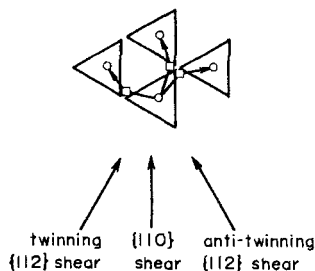
In the stable non-degenerate core configurations and in the split configurations for ϕ_{II} potentials, all the atomic interactions are harmonic since z_0 is small enough. This fact may be related to the equivalence of the energies in two types of configurations.

5.4. Non-degenerate core and slip behaviour of α -iron

As computer simulations in a previous paper (Takeuchi and Kuramoto 1975) have shown, even if the core structure is of non-degenerate type, the dislocation behaviour under stress at a given temperature is rather complex because of complicated modifications of the Peierls potential on application of stress and of the existence of the direct transition from one split configuration to another split configuration without passing through a non-degenerate configuration. To simplify the argument and to explain the slip behaviour in iron, we assume here that the Peierls potential between split configurations without passing a non-degenerate configuration is too high for the transition probability to be neglected. In such a case the movement of a dislocation core is rather simple; an elementary process of dislocation motion is the translation between two stable positions via a metastable position, as schematically shown fig. 7. In this case: (1) dislocations tend to glide along the most highly stressed $\{110\}$ plane; (2) asymmetry of slip for $\{112\}$ shear should occur because of the non-straight movement of the core (see fig. 7); and (3) a hump is expected to appear in the τ - T curve due to a camel hump Peierls potential, as shown by Guyot and Dorn (1967). Thus, all the characteristic features of slip in α -iron can be consistently interpreted by the non-degenerate type core.

In conclusion, it has been shown that the stable core of a screw dislocation in the b.c.c. lattice can be of non-degenerate type depending on the shape

Fig. 7



Schematic representation of the movement of a non-degenerate core from a stable position to another (marked by circles) via a metastable position (squares). Arrows show the directions of forces on the dislocation by application of the shear stresses indicated.

of the interatomic row potential and the non-degenerate core is always accompanied by the existence of the metastable split structure. Characteristic behaviour of slip in α -iron can reasonably be explained by such a non-degenerate core structure of the screw dislocation.

ACKNOWLEDGMENT

The author would like to thank Professor T. Suzuki for his interest and encouragement.

REFERENCES

- BASINSKI, Z. S., DUESBERY, M. S., and TAYLOR, R., 1971, *Can. J. Phys.*, **49**, 2160.
 CHRISTIAN, J. W., 1970, *Proceedings of the 2nd International Conference on the Strength of Metals and Alloys* (Cleveland: American Society of Metals), p. 31.
 CONTE, R., GROH, P., and ESCAIG, B., 1968, *Phys. Stat. Sol.*, **28**, 475.
 DUESBERY, M. S., VITEK, V., and BOWEN, D. K., 1973, *Proc. R. Soc. A*, **332**, 85.
 GUYOT, P., and DORN, J. E., 1967, *Can. J. Phys.*, **45**, 983.
 HEINRICH, R., and SCHELLENBERGER, W., 1971, *Phys. Stat. Sol. (b)*, **47**, 81.
 HIRSCH, P. B., 1968, *Trans. Japan Inst. Metals*, Suppl., **9**, xxx.
 HÜBNER, U., 1975, *Phys. Stat. Sol. (b)*, **67**, 113.
 KURAMOTO, E., MINAMI, F., and TAKEUCHI, S., 1974, *Phys. Stat. Sol. (a)*, **22**, 411.
 LEEMANS, D., and FINE, M. E., 1973, *Proceedings of the 3rd International Conference on the Strength of Metals and Alloys*, Vol. I (London: Institute of Metals), p. 510.
 MATSUI, H., MORIYA, S., TAKAKI, S., and KIMURA, H., 1978, *Trans. Japan Inst. Metals*, **19**, 163.
 MINAMI, F., KURAMOTO, E., and TAKEUCHI, S., 1972, *Phys. Stat. Sol. (a)*, **12**, 581; 1974, *Ibid.*, **22**, 81.
 QUESNEL, D. J., SATO, A., and MESHII, M., 1975, *Mater. Sci. Engr.*, **18**, 199.
 SEEGER, A., and WÜTHRICH, C., 1976, *Nuovo Cim.*, **33**, 38.
 SESTAK, B., and SEEGER, A., 1971, *Trans. Iron Steel Inst. Japan*, Suppl., **11**, 1283.
 SPITZIG, W. A., and KEH, A. S., 1970, *Acta metall.*, **18**, 611.
 SUZUKI, H., 1968, *Dislocation Dynamics*, edited by A. R. Rosenfield, G. T. Hahn, A. L. Bement and R. I. Jaffee (New York: McGraw-Hill), p. 679; 1970, *Fundamental Aspects of Dislocation Theory*, edited by J. A. Simmons, R. deWitt and R. Bullough (Washington: National Bureau of Standards (U.S.)), p. 253.
 TAKEUCHI, S., and KURAMOTO, E., 1974, *Phil. Mag.*, **30**, 319; 1975, *J. phys. Soc. Japan*, **38**, 480.
 TAKEUCHI, S., TAOKA, T., and YOSHIDA, H., 1969, *Trans. Iron Steel Inst. Japan*, **9**, 105.
 TSENG, D., and TANGRI, K., 1977, *Scripta metall.*, **11**, 719.
 VITEK, V., 1970, *Scripta metall.*, **4**, 725; 1974, *Crystal Lattice Defects*, **5**, 1; 1976, *Proc. R. Soc. A*, **352**, 109.
 VITEK, V., PERRIN, R. C., and BOWEN, D. K., 1970, *Phil. Mag.*, **21**, 1049.
 WÜTHRICH, C., 1977, *Phil. Mag.*, **35**, 325.